

Rover engineered to evaluate impacts of microclimatic parameters on pediatric asthma in Dallas schools

Joon Lee¹, Tae Lee¹

¹ Frisco High School, Frisco, Texas

SUMMARY

Pediatric asthma remains a significant health vulnerability for Dallas students due to atmospheric pollutants. While vegetation is known to lower pollution levels, the relationship between specific microclimatic (local atmospheric) and meteorological parameters and pediatric asthma rates in urban schools—and how vegetation modulates this relationship—is poorly understood. This study addressed this gap by examining the extent to which these parameters increase pediatric asthma vulnerability (PAV) in Dallas schools at the census tract level. We hypothesized that schools in census tracts with a lower normalized difference vegetation index (NDVI) would have a higher PAV compared to schools in more vegetated tracts due to increased exposure to microclimatic parameters, including particulate matter (PM), carbon monoxide (CO), and carbon dioxide (CO₂). Using a novel, cost-effective mobile rover with Arduino-based sensors, we measured these parameters at 3 sublocations in 10 Dallas schools on July 13th and 20th, 2024. In experimental schools with low NDVI, fine PM concentrations were 27% higher, coarse concentrations were 55% higher, CO was 2% higher, and CO₂ was 19% higher. By analyzing emergency department (ED) visits, chronic obstructive pulmonary disease (COPD) prevalence, and average inhaler prescription data to assess PAV, we found experimental schools had 78% more ED visits, 48% higher COPD prevalence, and 124% fewer inhaler prescriptions compared to control schools, suggesting that elevated PM and CO₂ concentrations are associated with increased PAV in census tracts of experimental schools, particularly in downtown and southeast Dallas. These findings are important for informing Dallas school policies governing atmospheric safety and healthcare equity.

INTRODUCTION

Despite remaining amongst the most prevalent and serious long-term diseases affecting children across the United States (US), pediatric asthma and its relationship with environmental exposures remains poorly understood. In 2020, asthma exacerbations affected approximately 25.2 million Americans, 4.2 million of whom were children, and accounted for over 986,000 emergency department (ED) visits across the US (1). Although environmental factors, particularly atmospheric pollution, are known to exacerbate

pediatric asthma symptoms, interactions between specific pollutants, microclimatic and meteorological conditions, and greenness in outdoor school environments remain poorly understood (2, 3).

While the factors contributing to pediatric asthma incidence, severity, and prevalence are numerous, studies relating to the correlation between pediatric asthma and environmental exposures in urban environments have primarily focused on aggregated factors contributing to asthma burden, notably traffic-related air pollution (TRAP), indoor allergens and microbes, and social determinants of health (SDOH) (4). Although a substantial body of research has statistically linked atmospheric pollutant parameters, such as particulate matter (PM) and nitrogen oxides (NO_x), to a higher asthma incidence, few studies have examined the effects of individual atmospheric pollutants, such as specific sizes of PM, in the context of their interactions with meteorological parameters—such as temperature, humidity, and wind speed—on pediatric asthma vulnerability (PAV) in the context of urban school environments at the census tract level (5). PAV refers to the increased risk of asthma-related health issues, such as ED visits and chronic respiratory conditions, in children due to environmental factors like air pollution (5). This makes it difficult to disentangle which specific microclimatic and meteorological parameters contribute to a rise in pediatric asthma morbidity and in what ways. Only a small number of studies have specifically investigated the correlation between pediatric asthma attacks and microclimatic conditions but have not conclusively determined whether these factors directly contribute to asthma exacerbations or if their impact is mediated through interactions with other environmental exposures, such as vegetation (6, 7).

PM is a complex mixture of microscopic airborne pollutants suspended in the atmosphere, typically classified by their aerodynamic diameter, with fine PM (>PM_{0.3}) referring to PM between 0.3 and 2.5 micrometers in diameter and coarse PM (>PM_{2.5}) referring to PM between 2.5 and 10.0 micrometers in diameter (8). Carbon dioxide (CO₂) is a colorless, odorless gas that contributes to the greenhouse effect and is produced through respiration, volcanic activity, or the burning of organic matter (9). Carbon monoxide (CO) is a gas formed when fossil fuels or biomass are combusted incompletely (10). A meteorological parameter is a measurement used to characterize the state of the weather at a specific location and time, including temperature (air warmth), humidity (moisture content), and wind speed (airflow velocity) (11).

Normalized Difference Vegetation Index (NDVI) is a remote sensing measure that quantifies vegetation density by comparing the difference between near-infrared and visible light reflected from the Earth's surface, with higher

NDVI values indicating greater vegetation cover. NDVI values sensitively reflect different forms of vegetation in proportion to their effects on meteorological parameters, such as canopy and shrub coverage, which more significantly influence local temperature regulation, air quality, and humidity than grass coverage (12). This sensitivity enables NDVI to capture meaningful variations in green space percentage, where specific increments indicate substantial increases in vegetation coverage, making it particularly relevant in urban environments with sparse vegetation (12). The NDVI value of 0.2 was used as a cutoff for inclusion in the experimental group in this study because it distinguishes areas with low vegetation, which are more susceptible to environmental stressors, from regions with moderate to high vegetation density to provide a clear threshold for assessing vegetation's impact on microclimatic parameters (12, 13). Unlike alternative indices, such as Enhanced Vegetation Index—which can be influenced by soil background and atmospheric conditions—NDVI's normalization process minimizes environmental noise from variable lighting, soil background, and topography, allowing for a more accurate, standardized method for assessing vegetation cover in a way that aids replication across regions and time periods (13).

The goal of this study is to clarify in what ways atmospheric parameters correlate with pediatric asthma prevalence in select Dallas Independent School District (DISD) schools at the census tract level. We hypothesized that DISD schools located in census tracts with lower NDVI values would have a significantly higher pediatric PAV as defined by a high rate of ED visits and chronic obstructive pulmonary disease (COPD) coupled with low inhaler prescription rates. This is because vegetation filters PM by absorbing it through leaves or trapping it in stomata, which can help reduce asthma risk. Without sufficient vegetation, pollutants like fine PM and coarse PM are more likely to remain suspended in the air, especially under unfavorable conditions such as higher wind speeds (14). Secondly, we hypothesized that this effect would be modulated by unfavorable meteorological parameters. Our study specifically explores this relationship by using a cost-effective, mobile rover engineered with Arduino-based aerial sensors to measure seven microclimatic parameters across three categories: PM (fine and coarse), carbon oxide (CO₂ and CO), and meteorological (temperature, humidity, and wind speed). We chose to measure these parameters because they are atmospheric indicators that could reveal how varying levels of urban greenness might influence the relationship between specific pollutants and meteorological conditions on PAV or were parameters that demonstrate measurable fluctuations within short time frames (e.g. hourly or daily) that could affect pediatric asthma symptoms (15, 16). We found that elevated levels of PM and CO₂ were strongly associated with increased PAV in census tracts of experimental schools with low NDVI values relative to those of control schools, particularly in downtown and south Dallas. These findings are important for informing DISD policies governing atmospheric safety and healthcare equity in schools located in areas with low vegetation cover to reduce PAV.

This study is the only effort to assess the impact of microclimatic parameters on PAV in Dallas and to mobilize cost-effective, aerial, and real-time sensors in school environments to our knowledge. The rover's portability and affordability make it a viable air quality monitoring (AQM)

tool for DISD schools by informing policy decisions tailored to each school's unique microclimatic conditions rather than a traditional reliance on climatic data averaged across a ZIP code. This rover overcomes the primary limitation of stationary sensors by actively mobilizing them to assess pollutant variability in a given location, rather than relying on fixed positions that must wait for pollutants to reach the sensor, thus increasing data accuracy and coverage. This study supports DISD schools' efforts to adopt an integrated AQM approach since it finds that schools with low NDVI and high PAV had poorer air quality based on PM and CO₂.

RESULTS

The goal of this study is to assess how microclimatic parameters, including PM and carbon oxide, and meteorological factors, correlate with PAV in DISD schools. We hypothesized that schools in census tracts with lower NDVI values would have significantly higher PAV. We gathered data on the selected microclimatic (fine PM, coarse PM, CO₂, and CO) and meteorological (air temperature, humidity, and wind speed) parameters at 10 selected DISD schools, divided into 5 experimental and 5 control locations to test our hypothesis (**Table 1**). Schools in census tracts with NDVI values less than 0.2 were classified as experimental locations, while schools in census tracts with NDVI values between 0.2 and 0.6 were classified as control locations. To control for environmental confounders such as time of day, seasonal variations, and local weather conditions, we collected 180 measurements from 3 designated sublocations—selected based on the largest parking lot (≥1,000 m²), the publicly accessible green area (≥5,000 m²), and the widest adjacent road by length—each with 3 replicates on July 13th and 20th, 2024. We measured our microclimatic and meteorological parameters with mobile Arduino-based sensors that transmitted atmospheric data to a laptop (**Figure 1**). For each location, we averaged the microclimatic parameters by aggregating data collected during the 3-minute trial period, with sensors recording every 10 seconds, yielding 18 data points per parameter per trial. We then used these data points for statistical analyses by performing an unpaired two-sample t-test for each parameter to ascertain statistical significance.

Label	Location type	Location
E1	Experimental	Billy Earl Dade Middle School
E2	Experimental	North Dallas High School
E3	Experimental	W.H. Adamson High School
E4	Experimental	Franklin D. Roosevelt High School
E5	Experimental	David W. Carter High School
C1	Control	Charles A. Gill Elementary School
C2	Control	Seagoville North Elementary School
C3	Control	Wilmer Hutchins High School
C4	Control	Francisco Medrano Middle School
C5	Control	H. Grady Spruce High School

Table 1: We took measurements at 10 locations. DISD schools in census tracts with NDVI values less than 0.2 were categorized into the experimental group (E1, E2, E3, E4, E5), while DISD schools in census tracts with NDVI values between 0.2 and 0.6 were categorized into the control group (C1, C2, C3, C4, C5).

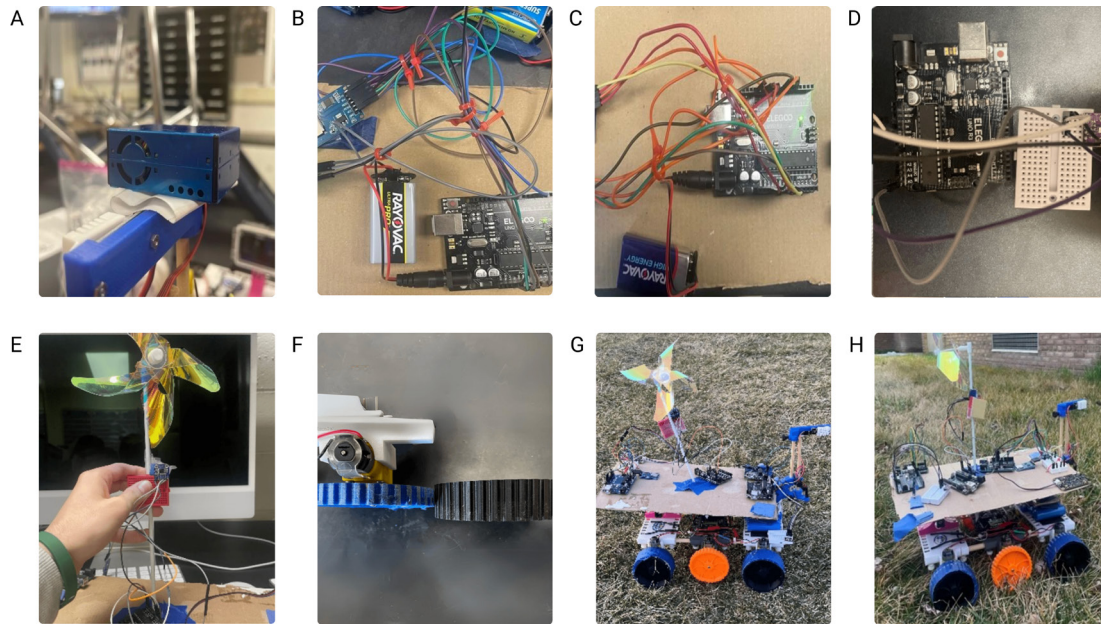


Figure 1: Rover construction with atmospheric sensors. We constructed a remote-controlled rover equipped with sensors for each selected atmospheric parameter using C++ in the Arduino IDE. (A) A PMS7003 sensor used to collect PM data, measured in particles per cubic meter (particles/m³). (B) An MQ-7 sensor used to collect CO data, measured in parts per million (ppm). (C) An MQ-811 sensor used to collect CO₂ data in ppm. (D) A BME280 temperature, humidity, and barometer sensor used to record temperature in Celsius (°C) and humidity as a percentage. (E) A modified VCNL4010 sensor connected to a handheld pinwheel used to collect wind speed data in kilometers per hour (kph) based on the number of spins counted while testing. (F) CAD 3D-printed wheels used for the rover. (G) The rover is equipped with atmospheric sensors and modified parts outdoors. (H) The deployment of the rover in a grassy schoolyard.

Experimental schools had significantly higher average PM concentrations than control schools for both fine PM ($p < 0.0001$) and coarse PM ($p = 0.0001$), with a more pronounced increase for coarse particles compared to fine particles. On average, fine PM concentrations on July 13th and 20th, 2024, for the experimental group were 1447.80 ± 15.700 particles/m³, while control group measurements were significantly lower at 1143.10 ± 22.100 particles/m³ (**Figure 2**). These results indicate that fine PM concentrations in experimental locations were approximately 27% higher than fine PM concentrations in control locations on July 13th and 20th, 2024 ($p < 0.0001$). To a greater degree, the average coarse PM concentration on July 13th and 20th, 2024, for the experimental group was 10.48 ± 0.600 particles/m³, while

control group measurements were significantly lower at 6.74 ± 0.160 particles/m³. This suggests that experimental locations had coarse PM concentrations approximately 55% higher than coarse PM concentrations in control locations.

Experimental schools recorded higher CO concentrations than control schools, though this difference was not statistically significant ($p = 0.44$). On average, CO concentrations on July 13th and 20th, 2024, were 1.94 ± 0.070 parts per million (ppm), while control group measurements were 1.91 ± 0.040 ppm (**Figure 3**). These results indicate that carbon monoxide levels in experimental locations were approximately 2% higher than carbon monoxide levels in control locations ($p = 0.44$). CO₂ concentrations were significantly higher in experimental locations than in control locations ($p < 0.0001$). On average, CO₂ concentrations on July 13th and 20th, 2024, for the experimental group were 384.67 ± 3.630 ppm, while control group measurements were lower at 322.07 ± 2.140 ppm, indicating that experimental locations showed 19% higher CO₂ concentrations compared to control locations ($p < 0.0001$) (**Figure 3**).

Temperatures were significantly elevated in experimental locations compared to control locations ($p < 0.0001$). On average, microclimatic temperature on July 13th and 20th, 2024, for the experimental group was 39.05 ± 0.250 °C, while control group measurements were moderately lower at 34.50 ± 0.160 °C (**Figure 4**). These results indicate that temperatures in experimental locations were approximately 13% higher than in control locations. Similarly, humidity levels were significantly higher in experimental locations compared to control locations ($p < 0.0001$). On average, humidity on July 13th and 20th, 2024, for the experimental group was $48.03 \pm 0.260\%$, while control group measurements were lower

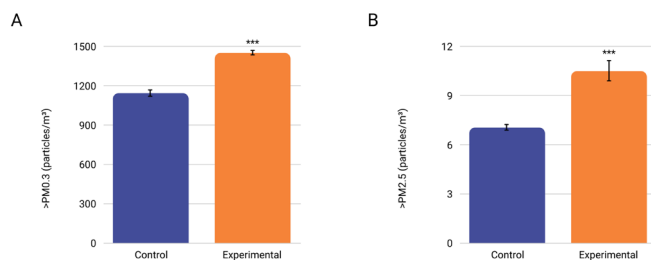


Figure 2: Experimental schools record significantly higher fine and coarse PM concentrations than control schools. Average (A) fine and (B) coarse measurements recorded from experimental school and control school (n=540/group). Error bars represent standard deviation. *** $p < 0.001$, derived from unpaired two-sample t-test for the average number of particles classified as fine PM and coarse PM in the experimental group compared to the control group.

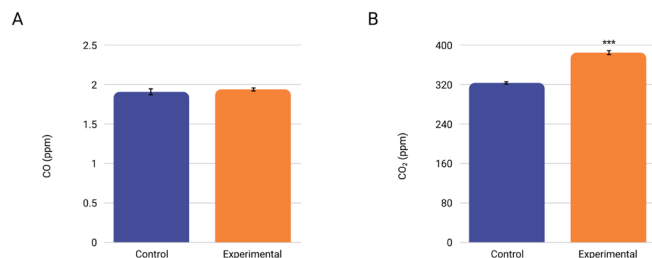


Figure 3: Experimental schools record similar CO concentrations and significantly higher CO₂ concentrations than control schools. Average (A) CO and (B) CO₂ measurements recorded from each experimental school and control school (n=540/group). Error bars represent standard deviation. ***p < 0.001, derived from unpaired two-sample t-test for the average CO₂ and CO concentrations in the experimental group compared to the control group.

at $38.58 \pm 0.310\%$ (Figure 4). These results indicate that humidity levels in experimental locations were approximately 20% higher than in control locations. Wind speeds were significantly higher in experimental locations compared to control locations ($p < 0.0001$). On average, wind speed on July 13th and 20th, 2024, for the experimental group was 13.07 ± 0.160 kilometers per hour (kph), while control group measurements were significantly lower at 11.42 ± 0.130 kph (Figure 4). These results indicate that wind speeds in experimental locations were approximately 14% higher than in control locations ($p < 0.0001$).

To acquire data on PAV, we used a publicly available asthma dataset by the Parkland Center for Clinical Innovation, compiled from its open data portal. This dataset provided information on the average number of ED visits caused by pediatric asthma per 90 days, the proportion of the population with COPD, and the average number of patients who were prescribed a pediatric asthma inhaler per year in each census tract in Dallas County (Figure 5) (17). Experimental schools had a significantly higher average number of ED visits ($p < 0.0001$), a significantly higher percentage of population with COPD ($p < 0.0001$), and a significantly lower number of inhaler prescriptions ($p < 0.0001$). The average number of ED visits was 53.16 for the experimental group and 29.89 for the control group; the percentage of the population with COPD was 11.06 for the experimental group and 7.47 for the control group; and the number of inhaler prescriptions was 73.58 for the experimental group and 164.60 for the control group. These results indicate that the highest PAV was in census tracts of experimental schools, where those with the highest average ED visits corresponded to a high COPD prevalence. In contrast, control tracts, with low PAV, indicated better asthma management, likely reducing severe cases. Spatially, experimental schools in downtown Dallas showed high PAV.

DISCUSSION

This study addresses the knowledge gap regarding the relationship between microclimatic parameters and PAV in DISD schools, focusing on how vegetation modulates exposure to atmospheric pollutants. We hypothesized that schools in census tracts with lower NDVI would experience higher PAV—as indicated by increased ED visits, higher COPD rates, and lower inhaler prescriptions—due to greater exposure to microclimatic parameters (fine PM, coarse

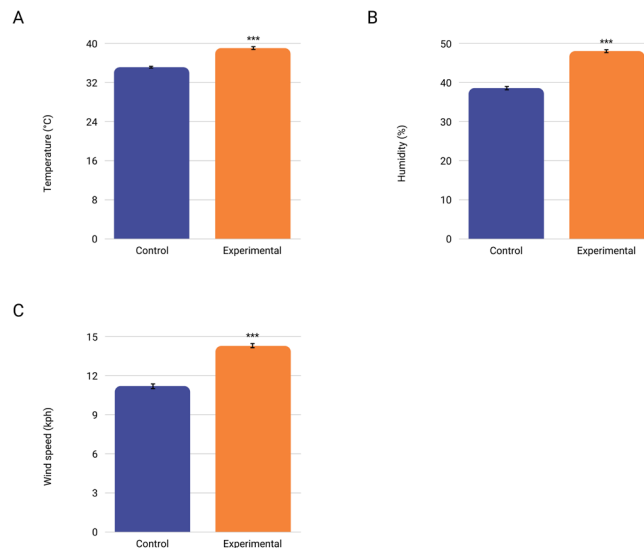


Figure 4: Experimental schools record significantly higher air temperature, humidity, and wind speed values than control schools. Average microclimatic (A) air temperature, (B) humidity, and (C) wind speed of the experimental group and control group on July 13th, 2024, and July 20th, 2024, averaged across dates, locations and sublocations from each experimental school and control school (n=540/group). Error bars represent standard deviation. ***p < 0.001, derived from unpaired two-sample t-test for the average microclimatic air temperature, humidity, and wind speed in the experimental group compared to the control group.

PM, CO, and CO₂), and potentially the interactions of those microclimatic parameters with meteorological parameters. Using a mobile rover with real-time sensors, we measured these pollutants and meteorological parameters across 10 schools and found that experimental schools with lower NDVI had significantly higher levels of PM and CO₂, which were strongly linked to increased PAV, especially in downtown and south Dallas.

Our results indicate that fine PM, coarse PM, CO₂, temperatures, humidity, and wind speeds are higher in experimental than control locations. This provides evidence that DISD schools in census tracts with lower NDVI values face greater exposure to these parameters and show a higher PAV compared to control tracts. Meteorologically, increased temperatures and humidity measured in experimental locations may also contribute to the higher PAV observed by exacerbating asthma symptoms due to increased allergen and air pollutant concentrations (18). This could explain the higher PAV, which is compounded by low inhaler prescriptions and barriers to healthcare access in experimental locations, compared to the cases observed in downtown areas. Higher wind speeds in experimental areas may increase the dispersion of airborne pollutants but could also result in less effective local pollutant trapping compared to areas with moderate vegetation cover, which typically has more vegetation to act as a natural barrier and reduce wind speed (19). This dynamic may contribute to the higher levels of pollutants and associated asthma risks in experimental locations.

Our results indicate that both fine—and, to a greater extent, coarse—PM concentrations were significantly elevated in

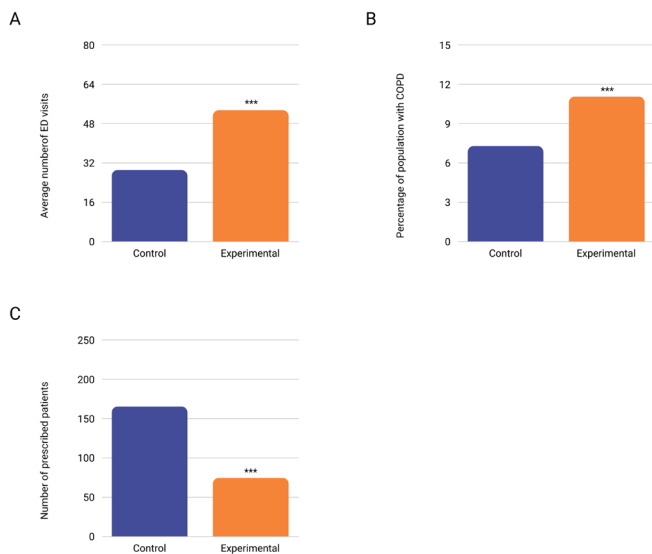


Figure 5: Census tracts of experimental schools record significantly higher PAV than census tracts of control schools. Average (A) number of ED visits caused by pediatric asthma per 90 days in experimental and control schools, (B) percentage of the population with COPD in experimental and control schools, and (C) number of patients prescribed a pediatric asthma inhaler per year in experimental and control schools. *** $p < 0.001$, derived from unpaired two-sample t-test for the average number of ED visits caused by pediatric asthma per 90 days in each school's census tract, the percentage of the population with COPD in each school's census tract, and the average number of patients prescribed a pediatric asthma inhaler per year in each school's census tract in the experimental group compared to the control group.

schools located in census tracts with low NDVI compared to those in control tracts with moderate NDVI. This provides evidence that schools in areas with lower vegetation cover could experience higher levels of fine and coarse PM in the DISD schools tested. Higher concentrations of fine, and, to a greater extent, coarse PM in experimental locations suggest that areas with lower vegetation cover experience elevated air pollutant levels. Vegetation filters and traps PM through their stomata or absorbs PM through leaves, after which it can be released through a process called resuspension, which is often dictated by wind speed (20). In areas with dense vegetation, PM is more likely to be captured before it can contribute to harmful exposure levels, while in low-vegetation areas, reduced filtration can result in higher coarse PM levels (20). The data indicates that coarse particles were elevated to a greater extent than fine particles, potentially because they are more easily trapped by vegetation due to their larger size. The lack of vegetation in experimental schools could allow larger particles to be suspended longer, increasing exposure. Higher CO₂ levels in experimental locations with low NDVI suggest a reduced capacity for natural CO₂ absorption and sequestration capabilities found in more vegetated environments. Vegetation naturally absorbs CO₂ from the atmosphere through photosynthesis by converting it into oxygen, which suggests that the lack of greenery in these areas potentially limits this absorption, leading to increased CO₂ accumulation and poorer air quality (21). The fact that CO values were not significantly higher in experimental locations than in control locations may have been a consequence

of a larger standard deviation brought on by a significant degree of data variability. Factors affecting CO variability may have been the presence or absence of CO-absorbing plant species, specifically *Sansevieria aureus* and *Scindapsus aureus*, which may have been more prevalent in control locations or have been less effective in experimental locations due to inadequate plant health or insufficient density (19). Additionally, significantly higher wind speeds in experimental areas could have increased dispersion of CO emissions from local sources, effectively diluting CO concentrations more at experimental sites than at control sites; consequently, this dispersion effect could mask the potential differences between sites if the experimental locations had higher, but more dispersed, CO sources (22). Furthermore, wind can cause turbulence and mixing of air layers, leading to the introduction of noise into the data and making CO concentration readings more variable (23). To determine the correlation between CO and PAV in areas with different NDVI values, further study is necessary.

Experimental schools recorded considerably higher microclimatic temperatures relative to that of control schools, suggesting that areas with low NDVI experience higher land surface temperature (LST) due to the urban heat island effect—the phenomenon where urban areas, due to dense infrastructure and reduced vegetation, experience higher LST compared to surrounding rural areas (24). Because urbanized areas show higher LST as urbanization replaces natural vegetation with impervious surfaces that absorb and retain heat, this inverse relationship between NDVI and LST suggests that areas with lower NDVI could experience less evapotranspiration and higher air temperatures, while areas with moderate NDVI benefit from greater vegetation, which provides shade and cooler microclimates, thereby mitigating temperature increases (25). Humidity levels were significantly higher in experimental locations, potentially due to reduced transpiration rates in areas with low NDVI, which can result in higher relative humidity and greater moisture retention as less moisture is released into the atmosphere (26). This results in higher surface temperatures, which increase evaporation rates from soil and water bodies, raising humidity levels (26). Wind speeds were significantly higher in experimental locations, potentially due to reduced surface roughness and less obstruction to wind flow by vegetation (27). In contrast, regions with moderate NDVI have denser vegetation that slows wind speeds (28). Given experimental locations experienced significantly higher temperatures, wind speed may have been affected, as air moves from high- to low-pressure areas driven by temperature changes (29). We chose to quantify urban greenness using NDVI because it allowed us to effectively isolate the impact of sparse vegetation on microclimatic conditions and PAV by modeling factors influencing vegetation health. This was particularly relevant in our study area, where localized variations in vegetation density significantly impact air quality and, in turn, PAV.

The findings of this study point to substantial policy implications for DISD schools, particularly those located in census tracts with elevated PM and CO₂ levels. Schools in census tracts in or peripheral to downtown Dallas should adopt more rigorous outdoor air quality (OAQ) interventions, which could include creating buffer zones of urban greenery in areas with high PAV to reduce local CO₂ concentrations and

create healthier microclimates to reduce PAV. On a municipal level, Dallas should partner with local healthcare providers to establish school-based asthma management programs in areas with high PAV to ensure students receive regular care and access to inhalers to reduce ED visits and democratize pediatric healthcare because fewer inhaler prescriptions in these tracts implied that many children may not receive adequate asthma management despite high PAV, potentially due to barriers in healthcare access or underdiagnosis. For example, tracts in the urban periphery—such as Experimental school 2 (E2), despite its proximity to downtown—showed a lower PAV, suggesting better access to management of chronic respiratory conditions, whereas experimental school 3 (E3) saw higher ED visits and higher COPD prevalence, indicating that areas can experience high PAV despite being geographically close to more stable regions. This suggests that while asthma management is more accessible than downtown, residents may be over-reliant on preventive medication due to localized environmental triggers rather than immediate health emergencies. Interestingly, control census tracts in Seagoville showed moderate ED visits and a low COPD prevalence but high inhaler prescriptions, while census tracts in North Dallas represented a lower-risk area for pediatric asthma, possibly due to more consistent access to healthcare services that prevents the kind of acute pediatric asthma incidents seen in higher-risk areas like South Dallas or the downtown core. The spatial inequity between these healthier northern tracts and more vulnerable southern regions indicates uneven exposure to environmental stressors and healthcare resources across Dallas. To improve the financial feasibility of these changes, DISD could jointly increase political investment for indoor air quality (IAQ) technology upgrades in older school facilities and OAQ interventions to improve student respiratory health outcomes (SRHOs) in environments where students spend much of their day and in those where they are exposed to the greatest volume of pollutants.

Several confounding factors should be considered in interpreting the findings of this study. For instance, the influence of SDOH, specifically higher poverty rates in experimental locations, is a confounding variable that could have affected results. High poverty levels correlate with increased rates of asthma due to limited healthcare access and poor living conditions, increasing PAV, independent of environmental exposures (30, 31). Furthermore, greater spatial accessibility to primary care pediatric services is associated with more scheduled primary care visits for asthma and fewer unscheduled ED visits, while limited access to care—correlated with poverty—often results in overreliance on emergency services, which can worsen SRHOs for disadvantaged urban children (32). Furthermore, variability in pollutant concentrations, particularly CO, may have been influenced by unmeasured local sources and wind effects. This indicates that while we observe higher parameter levels in experimental locations, a direct correlation between these parameters and PAV cannot be definitively concluded. Nonetheless, this study corroborates the significant correlation between low vegetation (low NDVI); elevated PM and CO₂ levels; and adverse meteorological conditions—higher air temperature, higher humidity, and higher wind speed—which collectively contribute to increased PAV in DISD schools.

MATERIALS AND METHODS

Site selection

Schools were selected for the experimental group based on five inclusion criteria (IC) and five exclusion criteria (EC) (Table 2). We chose these IC and EC to minimize confounding factors that could skew the relationship between urban greenness, air quality, and PAV. By selecting public schools in DISD with enrollment of over 500 students, we ensured a sufficiently large population to detect meaningful SRHOs. By limiting the study to schools located in census tracts with NDVI values between 0.2 and 0.6, we focused on areas with sparse but measurable vegetation. By excluding schools near ongoing construction and industrial projects, we aimed to mitigate the confounding effect of temporary spikes in PM and other pollutants. Proximity criteria ensured that schools were spatially distributed enough to avoid overlapping environmental exposures, while limiting our analysis to census tracts with five years of PAV data allowed for longitudinal reliability. Urban greenness was included as a criterion because it has been shown to influence air quality, temperature, and humidity, which affect asthma prevalence (33). NDVI, which measures vegetation density by comparing near-infrared and red light, was used to select schools in census tracts with low NDVI values (below 0.2) for the experimental group to isolate the impact of sparse vegetation on microclimatic conditions and PAV (34).

Out of 240 DISD public schools, 119 were excluded due to moderate NDVI values (0.2-0.6), as determined by the Google Earth Engine, which was configured to classify census tracts as having low (<0.2) or moderate (0.2-0.6) vegetation density. Landsat 8 Collection 1 Tier 1 surface reflectance imagery was processed to calculate NDVI for DISD school census tracts by selecting cloud-free images from the peak growing season (May 1 to September 30, 2023) and filtered to include only those within the geographic bounds of DISD. A cloud mask using the Quality Assessment (QA) pixel band was then applied to filter out clouds and shadows to exclude pixels classified as clouds, shadows, or cloud-adjacent using bitwise operators on the QA band. Only images with <5% cloud cover were included in the final dataset.

Number	Inclusion criteria (IC)	Exclusion criteria (EC)
1	Public schools designated as part of DISD for the 2023-2024 school year.	Schools located within 500 meters of an ongoing construction project.
2	Public schools in census tracts with average NDVI values less than 0.2.	Schools located in census tracts with average NDVI values between 0.2 and 0.6, inclusive.
3	Public schools in Dallas County census tracts with publicly available data on PAV for at least the past five years through the Parkland Center for Clinical Innovation open data portal.	Schools in census tracts where PAV data is missing or recorded for less than five years, as verified through the Parkland Center for Clinical Innovation open data portal.
4	Public schools with an enrollment of at least 500 students for the 2023-2024 school year.	Schools with an enrollment of fewer than 500 students for the 2023-2024 school year.
5	Public schools located greater than 3 miles apart from each other, measured from the center of each school's campus.	Schools located within a 3-mile radius of one another, measured from the center of each school's campus.

Table 2: Inclusion and exclusion criteria for the selection of DISD schools as part of the experimental group.



Figure 6: Selected experimental and control schools on a census tract map of DISD. The specified inclusion and exclusion criteria were applied to determine which DISD schools were part of the experimental group, while control schools were selected through stratified random sampling from five NDVI ranges (0.2 to 0.3, 0.3 to 0.4, 0.4 to 0.5, and 0.5 to 0.6).

Census tract boundaries were overlaid onto the NDVI map to calculate average NDVI values per tract. For census tracts extending beyond the DISD boundary, NDVI was calculated proportionally to their area in DISD. Further exclusions were made based on EC 1 (6), EC 3 (49), EC 4 (21), and EC 5 (35). Schools within a three-mile radius of each other were prioritized by larger enrollment, with the smallest enrollment excluded, resulting in eight schools for the experimental group. Control schools were selected through stratified random sampling from five NDVI ranges (0.2 to 0.3, 0.3 to 0.4, 0.4 to 0.5, and 0.5 to 0.6), resulting in five final control schools (Figure 6). Each school in the experimental and control groups was evaluated for 3 standardized sublocations: the largest parking lot ($\geq 1,000 \text{ m}^2$), publicly accessible green area ($\geq 5,000 \text{ m}^2$), and the widest adjacent road by length. Areas of potential sublocations were measured and compared using the polygon area measurement tool on Google Earth. Schools lacking any sublocation were excluded from the experimental group, resulting in the removal of three schools, while the control group remained unaffected. Data collection focused on the center of each sublocation, with the largest by area selected if multiple were present.

Calibration and data collection

To maximize data coverage and overcome the spatial limitations associated with traditional sensors, a novel, cost-effective, mobile rover engineered with sensors for each microclimatic parameter was used. A sturdy acrylic chassis was drilled to accommodate 4 high-torque DC motors, each secured with industrial screws and a 3D-printed, and a CAD modeled wheel (3.8 cm diameter) for optimal traction on various terrains. These motors were wired to an L298N motor driver (Bojack, BJ-L298N) controlled by an Arduino Uno REV3 microcontroller (Arduino, A000066), which was mounted on the chassis using plastic standoffs to reduce vibrations. Power for the rover was supplied by a rechargeable lithium-ion battery pack positioned beneath the chassis to maintain a low center of gravity for improved stability. Each sensor was

programmed using the Arduino programming language and IDE (version 2.3.2) and connected to the Arduino Uno REV3 (Arduino, A000066) mounted on a platform 0.25 meters above the ground, simulating a child's breathing zone (Figure 1). The PMS7003 sensor (LiebeWH, 671), MQ-7 sensor (Arduino, 12683), MQ-811 sensor (Ximimark, 430578031), BME280 sensor (HiLetgo, 13011231), modified VCNL4010 sensor (Adafruit, 466), and Arduino were wired onto a breadboard and secured with industrial tape and zip-ties to protect against dust and moisture. Wireless data logging was managed using SD card adapters linked to the Arduino Uno boards, with data transmitted via an HC-05 Bluetooth module to a paired laptop. Each sensor's library was imported into the Arduino IDE to enable communication and data was logged in real-time into a spreadsheet using Python scripts interfacing with the Bluetooth data stream.

At each of the 10 schools, the rover measured the microclimatic parameters at the 3 designated sublocations, with 3 replicates per sublocation, on July 13th and 20th, 2024, totaling 180 trials. These dates were selected to capture microclimatic variations under consistent summer meteorological conditions while avoiding confounding factors from active school operations. Sensors recorded data every 10 seconds for 3 minutes per trial in publicly accessible areas during open hours and non-operational days, per DISD policies. Each sensor held an SD card and an Arduino Uno for direct data storage during collection, which were transferred to a Microsoft Excel spreadsheet and organized by school, sublocation, date, and time. For each location, the microclimatic parameters were averaged based on the aforementioned 18 data points per trial, which were statistically analyzed by performing an unpaired two-sample t-test for each parameter to ascertain statistical significance from a Python-based statistical calculator (version 3.12.4) with the SciPy library (version 1.14.0) using the `scipy.stats.ttest_ind` function.

ACKNOWLEDGMENTS

We thank Dr. Jennifer Honda (Research Associate, University of Texas at Tyler) and Dr. Josh Banta (Research Associate, University of Texas at Tyler) for their guidance in this project.

Received: August 25, 2024

Accepted: November 29, 2024

Published: March 31, 2025

REFERENCES

1. "2020 Archived National Asthma Data." *Centers for Disease Control and Prevention*. www.cdc.gov/asthma/archivedata/2020/2020_archived_national_data.html. Accessed 7 Aug. 2024.
2. Hao, Hua, et al. "Daily Associations of Air Pollution and Pediatric Asthma Risk Using the Biomedical Real-Time Health Evaluation (BREATHE) Kit." *International Journal of Environmental Research and Public Health*, vol. 19, no. 6, 1 Jan. 2022, p. 3578, <https://doi.org/10.3390/ijerph19063578>.
3. Kudryavtseva, A.V. "The Impact of Atmospheric Pollution on Children's Respiratory Health." *Phdynasty.ru*, vol. 19, no. 2, 2024, <https://doi.org/10.20953/1817-7646-2023-2-136-144>.

4. Grant, Torie L., and Robert A. Wood. "The Influence of Urban Exposures and Residence on Childhood Asthma." *Pediatric Allergy and Immunology*, vol. 33, no. 5, 1 May 2022, <https://doi.org/10.1111/pai.13784>.
5. Zanobetti, Antonella, et al. "Early-Life Exposure to Air Pollution and Childhood Asthma Cumulative Incidence in the ECHO CREW Consortium." *JAMA Network Open*, vol. 7, no. 2, 28 Feb. 2024, <https://doi.org/10.1001/jamanetworkopen.2024.0535>.
6. Mireku, Nana, et al. "Changes in Weather and the Effects on Pediatric Asthma Exacerbations." *Annals of Allergy, Asthma & Immunology*, vol. 103, no. 3, 1 Sept. 2009, pp. 220–224, [https://doi.org/10.1016/S1081-1206\(10\)60185-8](https://doi.org/10.1016/S1081-1206(10)60185-8).
7. Rossi, O V, et al. "Association of Severe Asthma Attacks with Weather, Pollen, and Air Pollutants." *Thorax*, vol. 48, no. 3, 1 Mar. 1993, pp. 244–248, <https://doi.org/10.1136/thx.48.3.244>.
8. "Particulate Matter (PM) Basics." *United States Environmental Protection Agency*, www.epa.gov/pm-pollution/particulate-matter-pm-basics. Accessed 9 Aug. 2024.
9. "Carbon Dioxide Concentration" *National Aeronautics and Space Administration*, www.climate.nasa.gov/vital-signs/carbon-dioxide/?intent=121. Accessed 9 Aug. 2024.
10. "Basic Information about Carbon Monoxide (CO) Outdoor Air Pollution." *United States Environmental Protection Agency*, www.epa.gov/co-pollution/basic-information-about-carbon-monoxide-co-outdoor-air-pollution. Accessed 1 Sept. 2024.
11. "Meteorological Parameters." *European Environment Information and Observation Network*, www.eionet.europa.eu/gemet/en/concept/5195. Accessed 9 Aug. 2024.
12. Martinez, Alex, and S.M. Labib. "Demystifying Normalized Difference Vegetation Index (NDVI) for Greenness Exposure Assessments and Policy Interventions in Urban Greening." *Environmental Research*, vol. 220, no. 115155, 1 Mar. 2023, <https://doi.org/10.1016/j.envres.2022.115155>.
13. Zapata, Francisco, et al. "Why Normalized Difference Vegetation Index (NDVI)?" *Studies in Computational Intelligence*, vol. 1045, 23 Nov. 2022, pp. 83–92, https://doi.org/10.1007/978-3-031-08580-2_9.
14. Diener, Arnt, and Pierpaolo Mudu. "How Can Vegetation Protect Us from Air Pollution? A Critical Review on Green Spaces' Mitigation Abilities for Airborne Particles from a Public Health Perspective with Implications for Urban Planning." *Science of the Total Environment*, vol. 796, no. 148605, Nov. 2021, <https://doi.org/10.1016/j.scitotenv.2021.148605>.
15. Tong, Shilu, et al. "Exploring Atmospheric Environmental Drivers of Asthma among Children in Shanghai, China: Evidence-Informed Policies Are Required." *Advances in Climate Change Research*, vol. 14, no. 4, 1 Aug. 2023, pp. 587–591, <https://doi.org/10.1016/j.accres.2023.07.007>.
16. Wu, Chuansha, et al. "Associations of Early-Life Exposure to Submicron Particulate Matter with Childhood Asthma and Wheeze in China." *JAMA Network Open*, vol. 5, no. 10, 11 Oct. 2022, <https://doi.org/10.1001/jamanetworkopen.2022.36003>.
17. "2024 Dallas County Asthma Dataset." *Parkland Center for Clinical Innovation*, www.parklandhealth.org/2024-dallas-county-asthma-datset. Accessed 9 Aug. 2024.
18. Marcot, C. "Allergenic and Chemical Pollutants of Indoor Environments and Asthma: Characterization, Assessment and Expulsion." *Respiratory Diseases Review*, vol. 40, no. 7, Sep. 2023, <https://doi.org/10.1016/j.rmr.2023.06.001>.
19. Yan, Jingli, et al. "Uneven PM2.5 Dispersion Pattern across an Open-Road Vegetation Barrier: Effects of Planting Combination and Wind Condition." *Science of the Total Environment*, vol. 917, no. 170479, 20 Mar. 2024, <https://doi.org/10.1016/j.scitotenv.2024.170479>.
20. Lambers, Hans, and James Alan Bassham. "Photosynthesis." *Encyclopedia Britannica*, www.britannica.com/science/photosynthesis. Accessed 10 Aug. 2024.
21. Janah, Anisa, et al. "Absorption Pollutants Carbon Monoxide (CO) in the Air Using Sansevieria and Scindapsus Aureus." *Proceedings of the 5th International Conference on Science, Education and Technology*, vol. 29, no. 4, Jun. 2019, <https://doi.org/10.4108/eai.29-6-2019.2290383>.
22. Huang, Hong, et al. "A Two-Dimensional Air Quality Model in an Urban Street Canyon: Evaluation and Sensitivity Analysis." *Atmospheric Environment*, vol. 34, no. 5, Jan. 2000, pp. 689–698, [https://doi.org/10.1016/S1352-2310\(99\)00333-7](https://doi.org/10.1016/S1352-2310(99)00333-7).
23. "Turbulence." *Weather.gov*, 2019, www.weather.gov/source/zhu/ZHU_Training_Page/turbulence_stuff/turbulence/turbulence.htm. Accessed 10 Aug. 2024.
24. Bhowmik, Sharmistha, and Bindu Bhatt. "Spatiotemporal Analysis of Land Surface Temperature Owing to NDVI: A Case Study of Vadodara District, Gujarat." *Journal of Geomatics*, vol. 17, no. 1, 28 Apr. 2023, pp. 48–57, <https://doi.org/10.58825/jog.2023.17.1.83>.
25. Luo, Jianxing. "Study on the Impact of MODIS-Derived NDVI and NDBI on Land Surface Temperature." *Highlights in Science Engineering and Technology*, vol. 69, 6 Nov. 2023, pp. 249–258, <https://doi.org/10.54097/hset.v69i.11911>.
26. Dao, Gong. "Possible Impacts of Vegetation Cover on Local Meteorological Factors in Growing Season." *Climatic and Environmental Research*, vol. 13, no. 6, 1 Jan. 2008, <https://doi.org/10.3878/j.issn.1006-9585.2008.06.05>.
27. Arrogante-Funes, Patricia, et al. "Monitoring NDVI Inter-Annual Behavior in Mountain Areas of Mainland Spain (2001–2016)." *Sustainability*, vol. 10, no. 12, 23 Nov. 2018, pp. 4363–4363, <https://doi.org/10.3390/su10124363>.
28. Liu, Zhisong, et al. "Analysis of the Spatiotemporal Characteristics and Influencing Factors of the NDVI Based on the GEE Cloud Platform and Landsat Images." *Remote Sensing*, vol. 15, no. 20, 16 Oct. 2023, pp. 4980–4980, <https://doi.org/10.3390/rs15204980>.
29. Zhenxi, Shen. "Correlation Analysis between NDVI and Climatic Factors of Grassland Ecosystems in the Northern Tibetan Plateau from 1982 to 2003." *Resources Science*, vol. 31, no. 11, 1 Jan. 2009, <https://doi.org/10.5814/j.issn.1674-764x.2012.03.006>.
30. Bhat, Aarti C, and Andrew Fenelon. "Housing and Environmental Exposures: A Systematic Literature

- Review on Research and Policy Implications.” *Journal of Clinical and Translational Science*, vol. 7, no. s1, 1 Apr. 2023, pp. 123–124, <https://doi.org/10.1017/cts.2023.447>.
31. Kaur, Manpreet, et al. “Place and Pulmonary Health Inequality.” *Annals of the American Thoracic Society*, vol. 20, no. 10, 1 Oct. 2023, pp. 1400–1401, <https://doi.org/10.1513/annalsats.202308-669ed>.
 32. Teach, Stephen J., et al. “Spatial Accessibility of Primary Care Pediatric Services in an Urban Environment: Association with Asthma Management and Outcome.” *Pediatrics*, vol. 117, no. 2, Apr. 2006, pp. 78–85, <https://doi.org/10.1542/peds.2005-2000e>.
 33. Liu, Kun, et al. “Impact of Urban Forest and Park on Air Quality and the Microclimate in Jinan, Northern China.” *Atmosphere*, vol. 15, no. 4, 29 Mar. 2024, pp. 426, <https://doi.org/10.3390/atmos15040426>.
 34. “Measuring Vegetation (NDVI and EVI).” *National Aeronautics and Space Administration Earth Observatory*, earthobservatory.nasa.gov/features/MeasuringVegetation/measuring_vegetation_2.php. Accessed 12 Aug. 2024.

Copyright: © 2025 Lee and Lee. All JEI articles are distributed under the attribution non-commercial, no derivative license (<http://creativecommons.org/licenses/by-nc-nd/4.0/>). This means that anyone is free to share, copy and distribute an unaltered article for non-commercial purposes provided the original author and source is credited.